Published in final edited form as:
Anal Chem. 2007 March 1; 79(5): 2031–2036. doi:10.1021/ac061743r.

Oxidation Artifacts in the Electrospray Mass Spectrometry of Aβ Peptide

Maolian Chen and **Kelsey D. Cook***
Department of Chemistry, University of Tennessee, Knoxville, TN 37996-1600

Abstract

Gradual corrosion of stainless steel electrospray emitters under conditions of normal use generates surface irregularities that can promote electrical discharge. The increased emission current affects the electrochemical reactions associated with the spray process. When sampling the peptide Aβ(1–40), this is manifest by oxidation of methionine at position 35 to methionine sulfoxide. The resultant mass shift and reduced sensitivity can adversely affect H/D exchange experiments. These effects can be avoided by adding a redox buffer or (preferably) by re-polishing the emitter, especially to a rounded geometry.

Introduction

Under normal electrospray (ES) conditions, spray current (typically < 1 μA) is sustained by oxidation of solvent, emitter, or/and analyte. Individual species are generally oxidized in order of increasing redox potential until the required current is supplied [1]. If the electric field strength is too high, an electric discharge will occur, resulting in higher and less stable currents [2–3]. Production of reactive radicals can initiate a cascade of oxidation reactions in both the solution and gas phase [4–5]. While this effect can be enhanced by using an oxygen sheath gas and used to advantage in studies of the structure, dynamics, and interactions of (bio) macromolecules [6–10], in most applications the effects on analytical signals are deleterious.

Methionine is one of the most readily oxidized amino acid constituents of proteins [5,11–13]. Oxidation of methionine residues can result in significant conformational and/or functional changes [14], and thus represents an important posttranslational modification under conditions of oxidative stress or aging [15]. It is often therefore important to determine the amount of oxidized species in methionine-containing peptides and proteins. Although ES mass spectrometry (MS) can be a powerful technique for identifying and quantifying components in protein mixtures, spray-induced oxidation can complicate interpretation [5,16,17]. This report addresses the cause and means to control oxidation of the methionine-containing Aβ (1–40) peptide under “normal” ES conditions, as well as the dependence of oxidation on instrumental configurations.

Experimental Section

Materials

HPLC-grade acetonitrile (MeCN) and water were purchased from Fisher Scientific (Pittsburgh, PA). Tris(hydroxymethyl)aminomethane (tris), reagent-grade formic acid (95% in water), and porcine pepsin were purchased from Sigma Chemical (St. Louis, MO). Trifluoroacetic acid (TFA) was purchased from Pierce Biotechnology Inc. (Rockford, IL). Fused silica tubing was

*Correspondence should be addressed to Dr. Kelsey D Cook: e-mail: kcook@utk.edu; fax number: (865) 974-8019.

purchased from Polymicro Technologies (Phoenix, AZ). $H_2{}^{18}O$ (81.4% isotopic purity) was a generous gift from Dr. Albert A. Tuinman at the University of Tennessee.

Aβ(1–40) was purchased from Keck Biotechnology Center (Yale University, New Haven, CT) and purified according to the protocol described previously [18]. A 25-μM stock solution of Aβ monomer was prepared in 2 mM tris buffer (pH 7.5). Solutions and solvents were degassed by bubbling with nitrogen (boil-off from liquid N_2) for 5 min prior to MS analysis.

Electrospray Mass Spectrometry

A Q-Star XL quadrupole time-of-flight hybrid mass spectrometer (Applied Biosystems, Foster City, CA) was used to acquire ES mass spectra. The standard Q-Star IonSpray™ probe can be used in both a triaxial and a coaxial mode; details of these modes are provided elsewhere [19]. Diameters and flows for the various tubes were as indicated in Table 1. For both modes, sample and processing solvent flowed through silica capillaries to an external PEEK tee (Valco Instruments, Houston, TX) where they were mixed and delivered to the innermost tube of the probe, Tube 1. In the triaxial mode, MeCN pumped through the middle tube (Tube 2) was mixed with the sample/processing solvent mixture at the probe tip, resulting nominally in the same final composition as for the coaxial mode. Harvard Apparatus (South Natick, MA) syringe pumps were employed to deliver solutions.

Source parameters optimized for high sensitivity and stability were approximately the same for both modes. The emitter voltage and declustering potential were 4500 and 60 V, respectively. The sprayer tip was positioned about 12 mm away from the curtain plate and displaced about 5 mm off-axis at an angle of 45° to the ion sampling orifice. A microammeter (Model 27, Simpson Electric Co., Chicago, IL) was connected in series with the emitter to enable monitoring of the emission current. Nitrogen from liquid boil-off was used as nebulizer, curtain, and collision gas. Nebulizer and curtain gases pressures were 40 and 25 psi, respectively; the pressure in the collision cell was set at 3 or 5 (arbitrary units) for the MS and MS/MS modes, respectively. Mass spectra were acquired in the multichannel accumulation mode from 392 to 1200 m/z for 1 min (60 scans). MS/MS spectra were acquired using a 3 Da window for MS1 and collecting data from MS2 over the range 100–2000 m/z for 10 min (600 scans). Indicated uncertainties in relative intensities (or derived quantities) represent the standard deviation of 3 replicate spectra, each of which comprised 60 scans. To avoid interference from atmospheric moisture in hydrogen/deuterium exchange studies [19], the hole from the source leading to the venturi pump is generally blocked with a rubber stopper and nitrogen gas (500 mL/min, from boil-off) introduced into the source through the “make-up” hole in the source housing during and for 4 hours before sample injection. Although oxidation did not appear to be affected, this precaution was practiced here for consistency with earlier studies.

ProteinProspector 4.0.5 software (University of California, San Francisco) was used to identify possible matches for the oxidized and unoxidized ions of the proteolytic fragments obtained from the Aβ primary sequence. Assignments were confirmed using MS/MS with a collision energy of 30–45 eV.

High Performance Liquid Chromatography

Reversed-phase HPLC was conducted with a Hewlett Packard (Palo Alto, CA) 1100 system, using a ZORBAX SB-C3 column (3 mm × 150 mm) at 25 °C and a 100:1 splitter. The solvent flow rate was 1 mL/min. Solvent A was 0.1% TFA in water, and solvent B was 0.1% TFA in MeCN. The column was equilibrated to 1% solvent B prior to injection, and then the sample was eluted with a linear gradient from 1%–51% solvent B over a 40 min period. The separation was monitored by absorbance at 215 nm.

Tube Tip Polishing Procedure

A Dremel (Montreal, Canada) model 395 Moto-Tool equipped with a ¾ inch diameter medium sander disc was used to polish the tube tip. Polishing compound (#421, Dremel) was applied to the tip to help obtain a smooth rounded surface. After polishing, the tube was flushed with 500 μL of chloroform to remove any residual polishing compound, then rinsed with 500 μL of HPLC water and blown dry with nitrogen gas.

Scanning Electron Microscopy

Electron micrographs were obtained with a Hitachi (Schaumburg, IL) model S-3500N scanning electron microscope. X-ray fluorescence mapping was conducted using a Leo 1525 scanning electron microscope (Carl Zeiss SMT, Thornwood, New York). The magnification was 200 for the Hitachi microscope and 300 for the Leo microscope. The voltage was 20 kV on both microscopes.

Labeling data analysis

The extent of incorporation of ^{18}O into Aβ in experiments involving $H_2{}^{18}O$ was estimated by treating the experimental isotopic cluster as a linear combination of the cluster obtained with unlabeled water, and a hypothetical cluster for singly ^{18}O-labeled Aβ. The latter was modeled by shifting each peak in the unlabeled cluster upward by 2 Da (shifting m/z upwards by 2/z). This avoided the need for a fully labeled standard, and should be accurate so long as the sensitivities to the labeled and unlabeled Aβ are the same - a very reasonable assumption. All peaks in a given isotopic cluster were considered. (Note that the mass resolution was inadequate to distinguish isobars in the Aβ isotopic clusters, given its molecular weight of 4329.9 Da.)

Results and Discussion

Identification of Peptide Oxidation

Figure 1b shows a portion of an Aβ(1–40) mass spectrum obtained using emitter “A” after about 200 hours of spray time as the anode (Tube 2). In addition to the typical $[M+5H]^{5+}$ ion (base peak), another species with a similar isotopic pattern and with maximum intensity ~ 77% ± 3% (compared to the $[M+5H]^{5+}$ ion) is seen at a mass 16 Da higher than expected. This “heavy” peak was also observed for other charge states (+4: 78% ± 6%; +6: 82% ± 4%) (Figure 1a). On-line pepsin hydrolysis (as described in [19]) was undertaken to help identify the “heavy” peak. Seven fragments were observed: 1–19, 4–19, 20–33, 20–34, 34–40, 35–40 and 20–40. Among these, only fragments 34–40, 35–40 and 20–40 included peaks shifted by 16 Da, consistent with oxidation of the methionine residue at position 35. MS/MS analysis of the 16 Da heavier cluster from the singly charged 35–40 peptide produced a full series of b_n ions all shifted by 16 Da (data not shown), confirming that the methionine residue was indeed modified, probably by oxidative degradation prior to and/or during analysis by ES-MS [5, 16, 17].

The peaks attributable to oxidized species were much less intense in the coaxial mode (compare Figures 1b and 1c, both obtained with emitter A), and the emitter current was much lower (~2.2 μA) and more stable. The intensities in Figure 1c are consistent with the 4% relative abundance of the oxidized species evident from HPLC analysis; most of the oxidation evident in Figures 1a and 1b was apparently spray-induced.

Cause of Oxidation: Origin of the Oxygen Atom

Relatively high currents characterized by slow and random drift (6–12.6 μA over a period of 3 min) were observed during acquisition of Figures 1a and 1b, indicative of corona discharge [2–3]. Oxygen molecules have positive electron affinity and can readily capture thermal free

electrons in the discharge [20]. It was of interest to determine whether the oxygen atom inserted into Aβ derived from O_2 [5, 16, 17] (despite efforts to exclude room air), from other solutes, or from electrochemical oxidation of water.

To probe this chemistry, the experiment was repeated using ^{18}O-labeled water. Specifically, 4 μM Aβ monomer in 56/44/0.5 (v/v/v) $H_2O/H_2{}^{18}O$/HCOOH was pumped at 5 μl/min in Tube 1 in the triaxial mode, while 100/0.5 (v/v) MeCN/HCOOH was pumped at 5 μl/min in Tube 2, leading to a final water composition that was 44.1% ^{18}O. The oxidized peaks in the resulting mass spectrum (averaged over +4, +5, and +6 charge states) contained 42.6% ± 2.1% ^{18}O or ~ 96.6 % ± 4.8% of the expected 44.1%. Although this is within experimental error, the fact that the value is low is consistent with the HPLC evidence for ~ 4% contaminant present in the original sample (the contaminant presumably would not be ^{18}O labeled). Thus, water was clearly the oxygen source in these experiments. As in the "radical probe" experiments of Downard et al. [6–10], the extent of oxidation was inversely proportional to flow rate (data not shown). However, this could be due to simple dilution and current density effects. Thus, these experiments cannot resolve whether the oxidation takes place in solution or as a consequence of interactions with gas-phase radicals.

Regardless of mechanism, analyte oxidation can reduce sensitivity by distributing ion intensity among different ion signals. Solvent oxidation can also result in a dramatic change in the solution pH since the oxidation of water produces protons [21,22]. These electrochemically induced pH changes can cause protein unfolding if time allows [23]. For H/D exchange studies of proteins, the decrease in pH may result in more artifactual exchange [24] if the final pH deviates from the optimum value. Also, possible overlap of the partially deuterated peak with the oxidized peak can lead to imprecise determination of the number of incorporated deuterium labels. Furthermore, production of oxygen can form bubbles which adversely affect spray stability [25]. Minimization of the effect is desirable for all of these reasons.

Differences Between the Triaxial and Coaxial Modes

The higher current observed in the triaxial mode is consistent with the differences in effective electrode areas. In the coaxial mode, electrical contact is made only when the liquid from the inner silica Tube 1 wets the outer metal Tube 2; contact is essentially limited to the annular area at the tip of Tube 2 (~ 3.6×10^{-8} m^2). In the triaxial mode, the electrical contact area for the sample includes at least the final 5 mm inner surface of Tube 2 as well as the annular area of the tip, thus totaling ~ 3.5×10^{-6} m^2. While there is some uncertainty in these area estimations, the proportionate difference between them is surely greater than the ~5- to 6-fold difference in the emitter current (~2.2 *vs* 12.6 μA). Consequently, it is clear that the current density is higher in the coaxial mode: ~60 A/m^2, *vs* no higher than ~ 3.6 A/m^2 in the triaxial mode. Higher current density ordinarily signifies more aggressive conditions; other factors must contribute to the oxidation observed in the triaxial mode.

In light of the general difficulty of spraying pure aqueous solutions with conventional (as opposed to micro- or nanospray) emitters [26], one possible contributor to the excess oxidation in the triaxial mode is the imperfect mixing that is achieved in that mode [19]. To assess this contribution, Aβ samples were premixed to the same final composition as that used in the coaxial probe (50.5/49.5/0.46 water/MeCN/formic acid), then pumped through both Tubes 1 and 2 with the probe in the triaxial configuration. The resulting current was ~ 2.2 μA and the oxidation extent was similar to that observed in the coaxial mode (~ 4%). Similar results were obtained when the premixed solution was delivered only through Tube 2; imperfect mixing clearly enhances oxidation in the triaxial mode. Another contributor may be the effect of the silica Tube 1 on the field at the probe tip in the coaxial mode.

Progression of Oxidation

Oxidation became more pronounced as emitter A aged. By 300 hours of use, the maximum current increased to 13.5 μA (vs. ~12.6 μA at 200 h), and the oxidized peak became the base peak (relative abundance of the unoxidized peak was ~ 90% ± 3%; Figure 2a). Installing a new emitter (emitter B; Figure 3a) reduced the relative abundance of the oxidized peak to ~ 5.2% ± 0.1% with an emission current of ~ 0.2 μA (stable). The changes in performance of this emitter were monitored over a long period; they are summarized in Table 2. For this emitter, the $[M+5H+16]^{5+}$ ion became the base peak after ~ 150 h.

Control of Oxidation

Use of redox buffers—The effectiveness of a redox buffer [27] was tested with tris(2-carboxyethyl) phosphine (TCEP). TCEP was chosen because it has been reported to be a stronger reducing agent (and therefore potentially a more effective redox buffer) than the commonly used dithiothreitol (for which $E° = -0.110$V vs. SHE at pH 7; a corresponding value for TCEP could not be found) [28,29]. Using emitter A in the triaxial mode after ~ 200h use, addition of 100 μM TCEP to the 0.5% formic acid processing solvent reduced the $[M + 5H +16]^{5+}$ ion from 77% ± 3% to 6.2% ± 0.3% of the $[M + 5H]^{5+}$ base peak, but the emission current remained the same. After ~ 300h use, more TCEP (~ 150 μM) was required to decrease the oxidized peak to ~ 6% of the unoxidized peak, reflecting the further deterioration of the emitter and the increased tendency toward oxidation. Such high concentrations of TCEP can contaminate the ion source. Furthermore, suppression effects are common in ES [26]; 100 μM TCEP reduced the sensitivity to Aβ by ~ 13% (based on the sum of the intensities of oxidized and unoxidized peaks). Use of the redox buffer also risks reaction with Aβ to alter its structure and/or affecting the activity of enzymes used for on-line proteolysis. Thus, it would be better to eliminate the discharge, rather than ameliorate its symptoms.

Reduction of electric field—Smoothing a rough tip surface reduces the electric field gradient and therefore the discharge. As shown in Figure 2, oxidation was essentially eliminated after polishing the tip of emitter A; the current dropped to ~ 0.2 μA and the oxidized peak intensity fell to ~ 5.2 % ± 0.1% of the $[M+5H]^{5+}$ base peak. Polishing emitter B after ~ 150 h use had a similar effect (Table 2).

Note that oxidation with unpolished emitter B was much worse after 150 hours than it was after 300 hours using emitter A. In general the lifetime of emitters was observed to depend somewhat on the shape of the emitter tip. After polishing emitter A to the shape of Figure 2b, the oxidation remained under control (~ 5.4 ± 0.3% relative abundance for the oxidized species) after an additional ~ 165 h of use (Figure 4a), and the emitter current had increased only to ~ 0.4 μA (from 0.2 μA). Similarly, oxidation with emitter C (Figure 4b) increased from ~5.0% ± 0.2% to ~8% ± 1% during its first 140 h of usage, while current increased from ~0.2 to ~2.6 μA. By contrast, the relatively square-cut emitter B (Figure 3) showed ~11% ± 1% relative abundance for the oxidized species after being used for only ~ 50 h, increasing to ~ 51 % ± 4% after ~ 100 h of usage and to ~256% ± 3% after ~ 150 h of usage. Rounded emitters appear to have a higher resistance to corrosion, perhaps because this surface shape reduces the electrical field, and therefore the discharge.

The pits on the corroded surfaces evident in the micrographs suggest that segregation or preferential depletion of specific metal elements may take place as corrosion proceeds. However, X-ray fluorescence maps of emitter B after ~ 100 h in service showed that the distribution of major elements (such as Fe, Ni, Cr, Mo) was uniform (data not shown). The pits may simply result from the random attack of the tip surface by the reactive plasma generated during discharge.

Conclusions

The electrochemical properties of electrospray mass spectrometry must be considered when using the technique. In this study, oxidation of a methionine residue was promoted by an electrical discharge resulting from an eroded emitter. One straightforward consequence is loss of sensitivity due to dilution of the signal over more than one species. In H/D exchange studies, further complications can result from the mass increase unrelated to deuterium.

All the tested stainless steel tubes were vulnerable to discharge which resulted in corrosion. Since the magnitude of oxidation increases as the emitter ages, the addition of a reducing agent is not an ideal way to control oxidation. Polishing the tube helps prevent discharge and reduces its effects. Monitoring current provides a convenient way to diagnose the presence of discharge (current typically > 1 μA) and the need for tube polishing or replacement.

Although not investigated in this study, another way of suppressing discharge could be the elimination of electrons produced during discharge by flushing the space around the spray tip with an electron scavenging gas such as SF_6 or CO_2, or by the addition of a halogenated solvent to the liquid stream [20]. The converse approach of swamping the effect by using O_2 sheath gas (as in “radical probe MS” [6–10]) may complicate interpretation of H/D exchange data.

References

1. Van Berkel GJ, Zhou F. Anal. Chem 1995;67:2916–2923.
2. Yamashita M, Fenn JB. J. Phys. Chem 1984;88:4451–4459.
3. Yamashita M, Fenn JB. J. Phys. Chem 1984;88:4671–4675.
4. Van Berkel GJ. J. Mass Spectrom 2000;35:773–783. [PubMed: 10934431]
5. Morand K, Talbo G, Mann M. Rapid Commun. Mass Spectrom 1993;7:738–743. [PubMed: 8374164]
6. Maleknia SD, Chance MR, Downard KM. Rapid Commun. Mass Spectrom 1999;13(23):2352–2358. [PubMed: 10567934]
7. Maleknia SD, Downard KM. Mass Spectrom. Rev 2001;20(6):388–401. [PubMed: 11997945]
8. Wong JWH, Maleknia SD, Downard KM. Anal. Chem 2003;75(7):1557–1563. [PubMed: 12705585]
9. Shum W, Maleknia SD, Downard KM. Anal. Biochem 2005;344(2):247–256. [PubMed: 16091281]
10. Issa S, Downard KM. J. Mass Spectrom 2006;41(10):1298–1303. [PubMed: 17013829]
11. Chowdhury SK, Eshraghi J, Wolfe H, Forde D, Hlavac AG, Johnston D. Anal. Chem 1995;67:390–398. [PubMed: 7856883]
12. Kotiaho T, Eberlin MN, Vainiotalo P, Kostiainen R. J. Am. Soc. Mass Spectrom 2000;11:526–535. [PubMed: 10833026]
13. Guan Z, Yates NA, Bakhtiar R. J. Am. Soc. Mass Spectrom 2003;14:605–613. [PubMed: 12781462]
14. Brot N, Weissbach H. BioFacfors 1991;3:91–96.
15. Hong J, Schöneich C. Free Rad. Biol. Med 2001;31:1432–1440. [PubMed: 11728815]
16. Bateman KP. J. Am. Soc. Mass Spectrom 1999;10:309–317.
17. Kelly JF, Ramaley L, Thibault P. Anal. Chem 1997;69(1):51–60.
18. Kheterpal I, Zhou S, Cook KD, Wetzel R. Proc Natl. Acad. Sci. U S A 2000;97:13597–13601. [PubMed: 11087832]
19. Chen M, Kheterpal I, Wetzel R, Cook KD. J. Am. Soc. Mass Spectrom. 2007In Press.
20. Kebarle, P.; Ho, Y. Electrospray Ionization Mass Spectrometry: Fundamentals, Instrumentation and Applications. Cole, RB., editor. New York: John Wiley and Sons; 1997. p. 3-63.
21. Van Berkel GJ, Zhou F, Aronson JT. Int. J. Mass Spectrom. Ion Proc 1997;162:55–67.
22. Zhou S, Edwards AG, Cook KD, Van Berkel GJ. Anal. Chem 1999;71:769–776.
23. Konermann L, Silva EA, Sogbein OF. Anal. Chem 2001;73:4836–4844. [PubMed: 11681459]
24. Smith DL, Deng Y, Zhang Z. J. Mass Spectrom 1997;32:135–146. [PubMed: 9102198]
25. Moini M, Cao P, Bard AJ. Anal. Chem 1999;71:1658–1661. [PubMed: 10221079]

26. Cech NB, Enke CG. Mass Spectrom. Rev 2001;20:362–387. [PubMed: 11997944]
27. Lingane, JJ. Electroanalytical Chemistry. 2nd ed.. New York: Interscience; 1958.
28. Celland WW. Biochem 1964;3:480–482. [PubMed: 14192894]
29. Graham DE, Harich KC, White RH. Anal. Biochem 2003;318(2):325–328. [PubMed: 12814640]

Acknowledgments

This work was supported in part by the National Institutes of Health (grant no. R01-AG18927) and by the National Science Foundation (grant no. CHE-0130752). The authors are grateful to Dr. Albert A. Tuinman and Dr. Indu Kheterpal for helpful discussions.

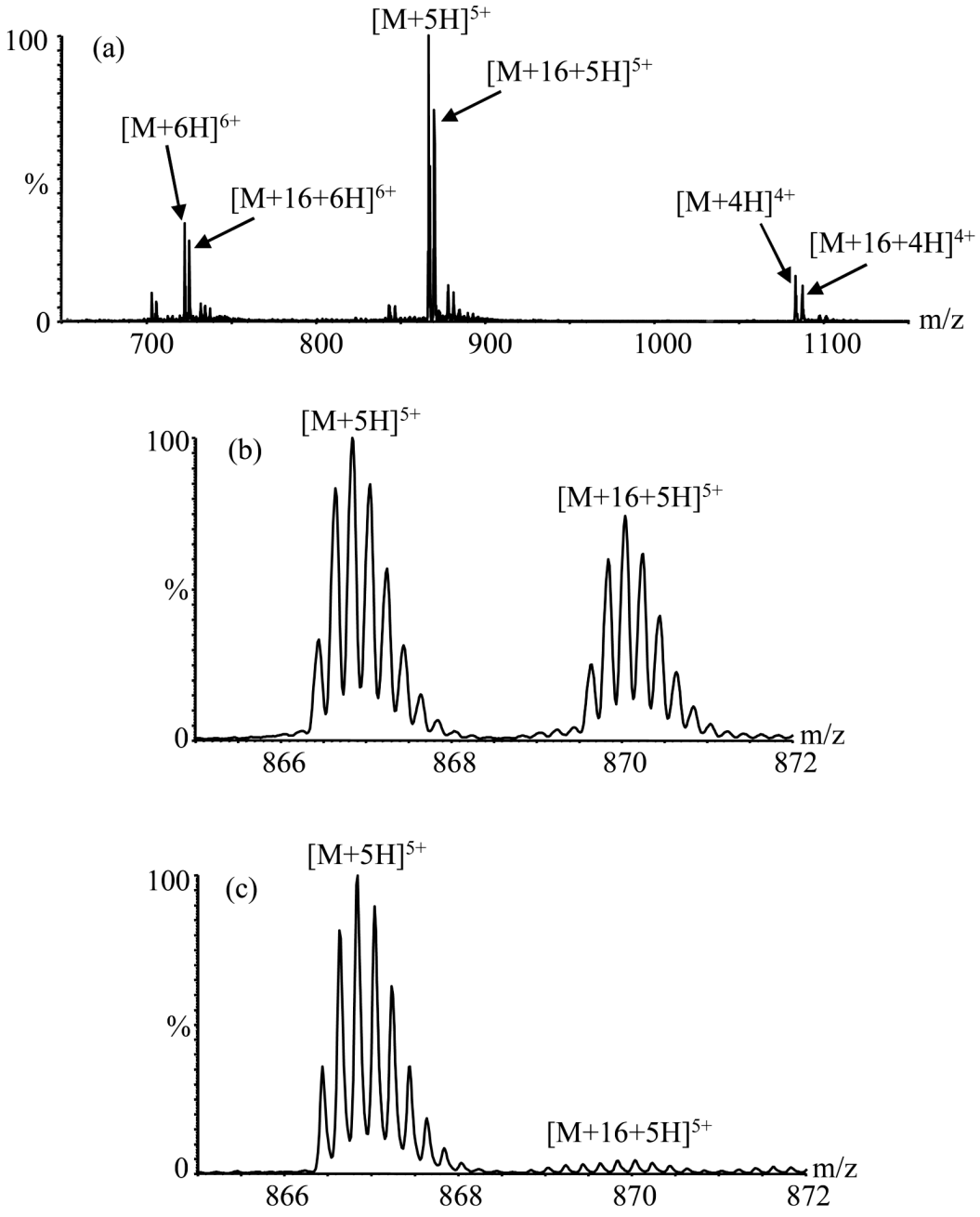

Figure 1.

ESI mass spectra of Aβ(1–40) peptide obtained using emitter A after 200 h in use. (a) Triaxial mode; full spectrum showing +4, +5, +6 charge states. (b) Detail from part (a) showing +5 charge states. (c) Coaxial mode showing +5 charge state. M is the molecular mass of the peptide.

(a) Before polishing

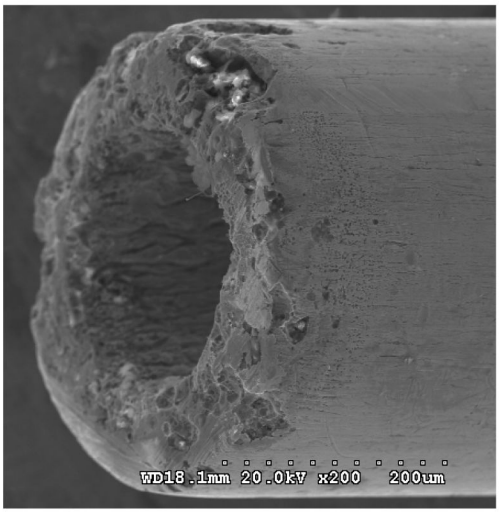

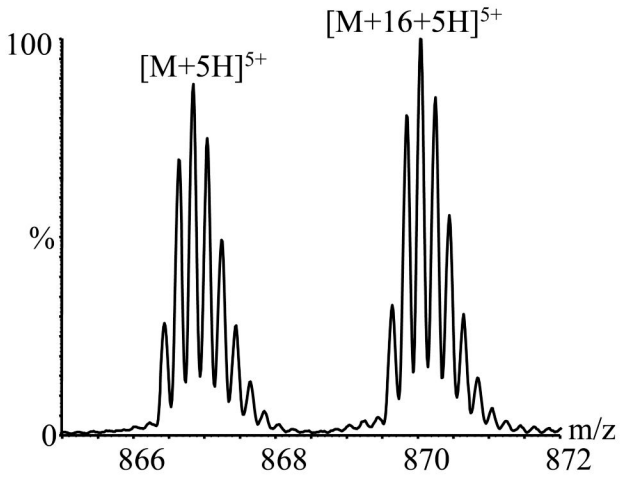

(b) after polishing

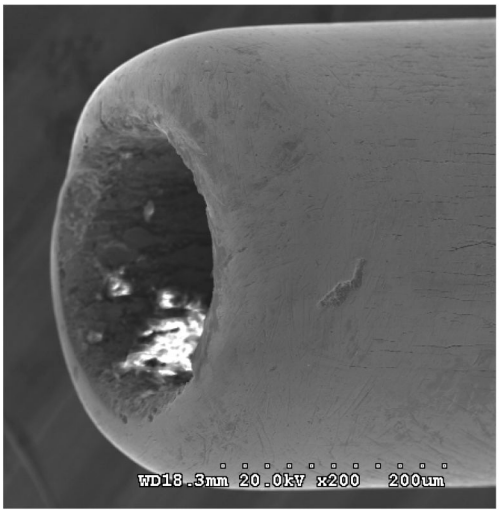

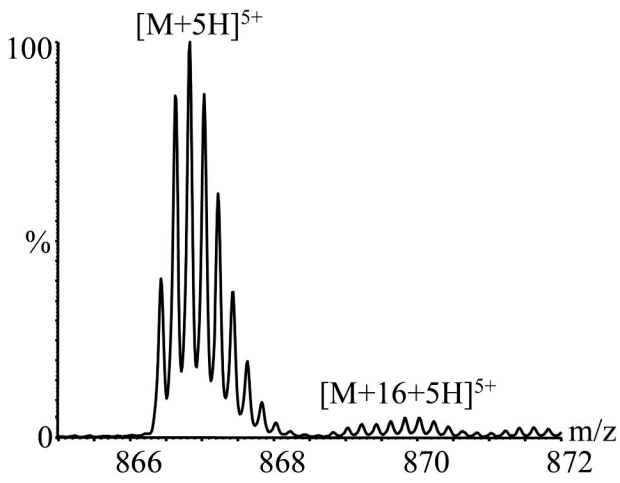

Figure 2.
Electron micrographs of emitter A and mass spectra acquired with it in the triaxial mode after ~ 300 h use: (a) before polishing; (b) after polishing.

(a) < 1 h in service

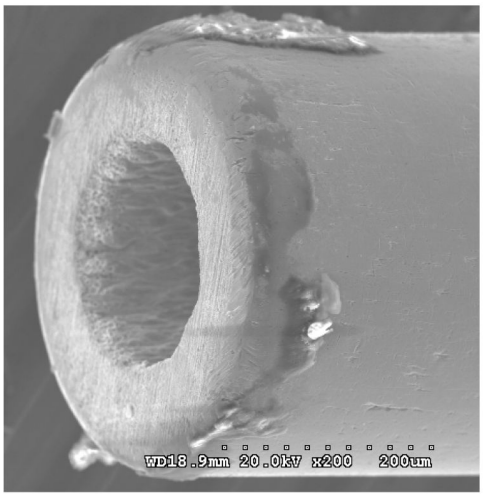

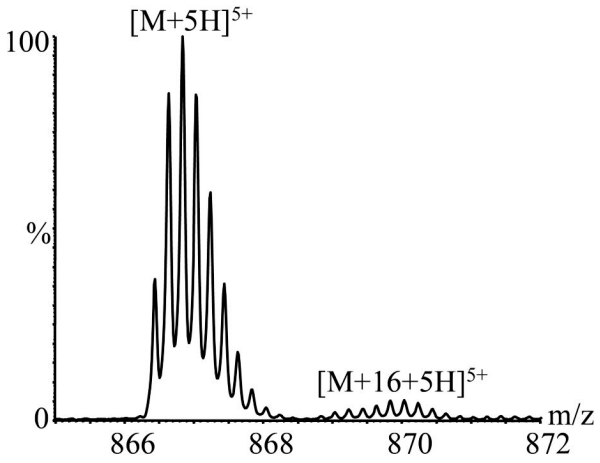

(b) ~ 100 h in service

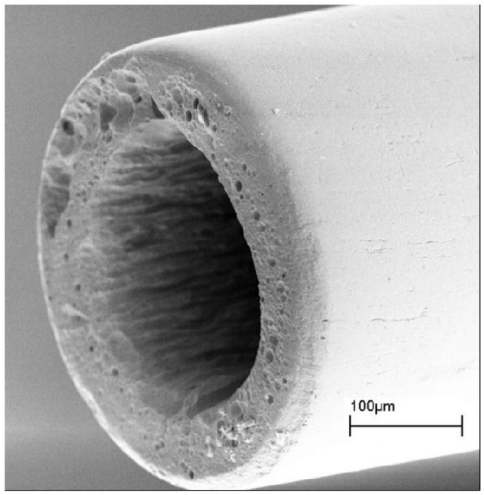

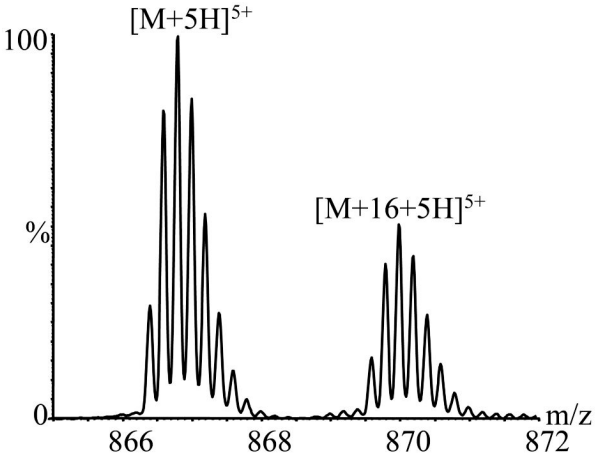

Figure 3.
Electron micrographs of emitter B and mass spectra acquired with it in the triaxial mode after (a) < 1 h in service; (b) ~ 100 h in service.

(a)

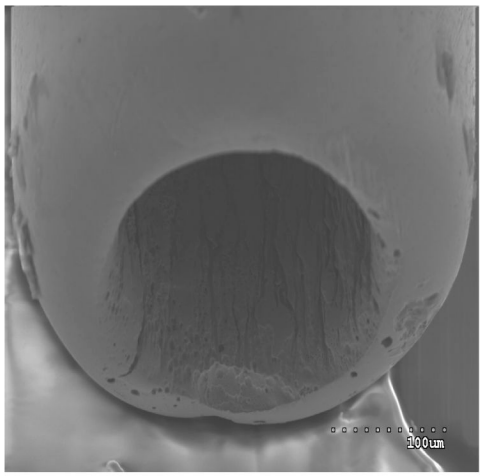

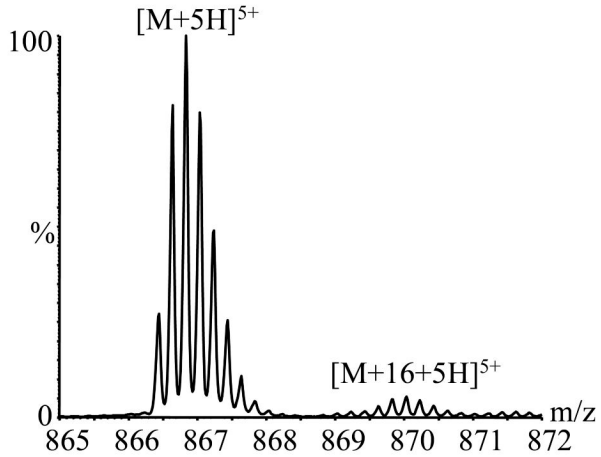

(b)

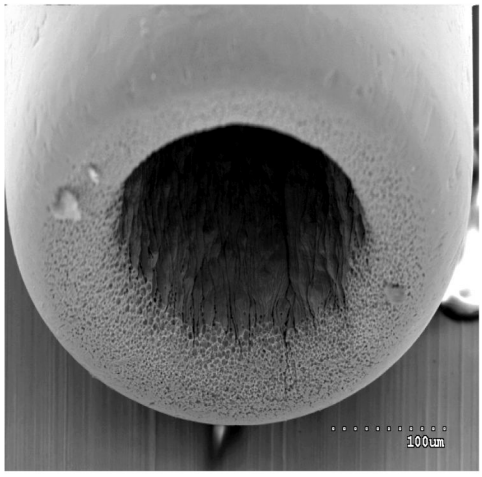

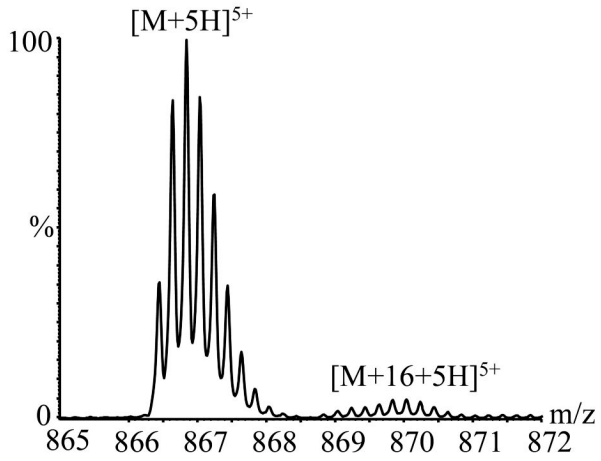

Figure 4.
Electron micrographs and associated mass spectra (triaxial mode) acquired using: (a) polished emitter A in service for ~ 165 h after polishing; (b) emitter C in service for < 1 h.

Table 1

Tube materials, dimensions (i.d. × o.d. × length), and flows for the IonSpray™ probe used in the coaxial and triaxial modes. Length is specified only for Tube 1, since that dimension (plus the flow rate) controls the time for mixing the sample and processing solvent.

	Coaxial Probe[1]	Triaxial Probe[2]
Tube 1	Fused silica: 75 μm × 190 μm × 46 cm 0.85 μL/min sample + 9.25 μL/min processing solvent[3]	Fused silica: 75 μm × 190 μm × 23 cm 0.85 μL/min sample + 4.25 μL/min processing solvent[4]
Tube 2 (anode)[5]	Stainless steel: 220 μm × 420 μm (No flow)	Stainless steel: 220 μm × 420 μm 5 μL/min MeCN (0.5% v/v formic acid)
Tube 3	Stainless steel: 510 μm × 820 μm N_2 sheath gas @ 40 psi	Stainless steel: 510 μm × 820 μm N_2 sheath gas @ 40 psi

[1] For the coaxial probe, the emitter ends of Tubes 1 and 2 are flush with one another.

[2] For the triaxial probe, Tube 1 is drawn ~ 5 mm back from the emitter tip of Tube 2, creating a mixing volume of ~ 0.19 μL.

[3] Processing solvent for the coaxial probe was 46/54/0.5 (v/v/v) water/MeCN/formic acid.

[4] Processing solvent for the triaxial probe was 0.5 % (v/v) formic acid in water.

[5] Tube 2 protrudes ~ 0.5 mm beyond the end of Tube 3.

Table 2

Performance of emitter B after various periods of use.

Hours of use	Emitter current (μA)	$[M+16+5H]^{5+}/[M+5H]^{5+}$
<1 (New)	0.2	0.052 ± 0.001
50	1 – 5[1]	0.11 ± 0.01
100	5 – 11[1]	0.51 ± 0.04
150	7 – 20[1]	2.57 ± 0.2
150 (Polished)	0.2	.050 ± 0.002

[1] Current drifts over the indicated range during the period of data acquisition